表 2　プリオン病の予防・治療薬候補として報告されている化合物(文献[4-8]他から引用)

| 化合物 | *in vitro* $PrP^{res}$ *a転換 *b | *ex vivo* $PrP^{res}$ 産生抑制 *c | *in vivo* 潜伏期延長 *d | コメント |
|---|---|---|---|---|
| ポリアニオン<br>(ペントサンほか) | 刺激 | Yes | Yes | 末梢における複製阻害<br>内因性グリコサミノグリカンと $PrP^{C}$ との相互作用阻害<br>脳室内投与で効果<br>ヒトで他の目的に使用 |
| スルフォン化色素<br>(コンゴレッドほか) | 抑制 | Yes | Yes | $PrP^{C}$ および $PrP^{res}$ に結合<br>内因性グリコサミノグリカンと $PrP^{C}$ との相互作用阻害 |
| テトラピロール | 抑制 | Yes | Yes | ヒトで他の目的に使用 |
| アントラサイクリン<br>(IDOX ほか) | | | Yes | 他のアミロイドーシスで報告あり |
| LTβR-Ig *e | | | Yes | 脾で $PrP^{res}$ や感染性を抑制 |
| ダプソン | | | Yes? | 抗炎症作用．$PrP^{res}$ 沈着に効果なし |
| ポリエン系抗生物質<br>(アムホテリシン B ほか) | 抑制 | | Yes | ヒト患者での有効性の報告なし |
| 分枝ポリアミン | | Yes | Yes *f | βシート構造を減少 |
| システインプロテアーゼ<br>インヒビター | 効果なし | Yes | | $PrP^{C}$ には影響なし |
| ヘパラン硫酸関連物質 | | Yes | Yes | 内因性ヘパラン硫酸と競合 |
| アクリジン誘導体<br>(キナクリン，クロロキン) | 効果なし | Yes | | 株依存性の効果．$PrP^{C}$ には影響なし |
| フェノチアジン系薬物<br>(クロルプロマジン) | | Yes | Yes | 構造上アクリジン誘導体に類似 |
| スラミン | | Yes | Yes | $PrP^{C}$ の代謝に影響 |
| テトラサイクリン | $PrP^{res}$ 減少 | | Yes | $PrP^{Sc}$ と結合 |
| β-ブレーカーペプチド | | | Yes | βシート構造を減少 |
| 合成 PrP ペプチド | 抑制 | Yes | | $PrP^{C}$ の $PrP^{res}$ への結合を阻害 |
| 抗 PrP 抗体 | 抑制 | Yes | Yes *f | 細胞膜上の $PrP^{C}$ に結合 |
| 銅キレート剤<br>(D-ペニシラミン) | 抑制 *g | | Yes | 血中および脳の銅減少 |

*a $PrP^{res}$：プロテアーゼ抵抗性の異常プリオン蛋白，*b *in vitro*：無細胞系でのプリオン蛋白転換実験，*c *ex vivo*：プリオン持続感染細胞実験，*d *in vivo*：プリオン病動物モデルでの実験，*e LTβR-Ig：lymphotoxin β-receptor-IgG fusion protein，*f：化合物で処理した感染細胞を投与した場合，プリオン病が伝播せず，*g：銅による PrP 転換増強効果を抑制．

アランス促進(図 2-⑦)まで含まれる．

*In vitro* の無細胞系でのプロテアーゼ抵抗性 PrP への転換実験，プリオン持続感染細胞を用いた実験，プリオン病動物モデルを用いた研究結果により，プリオン病の予防・治療薬候補として報告されている化合物を表 2 にあげた[4-8]．キナクリン，クロルプロマジンなど，すぐに使用可能ないくつかの既存の薬物[8]はヒトでの応用が試みられているが，現在までにヒトのプリオン病に有効であることが実際に検証されたものはない．

こうした化合物の臨床応用を考える場合，いくつかの点を念頭におく必要がある．ひとつは治療のタイミングの問題である．たとえば，硬膜移植後の CJD が約 10 年の潜伏期間を経て発症することからもわかるように，疾患は非常に長い潜伏期間のあとに発症し，いったん発症するときわめて急激な経過をたどる．臨床的に CJD の典型像を示す段階では脳は荒廃した状態になっており，治療はすでに手遅れである．したがって，治療薬が有効に使用されるためには発症前に，あるいは発症のごく早期に正確な診断が下される必要がある．また vCJD など，末梢での $PrP^{Sc}$ 複製が中枢神経系へ $PrP^{Sc}$ が伝播する前の必要なステップである場合には，末梢段階での制御が治療の重要な標的となる．また，中枢神経系における $PrP^{Sc}$ 複製を標的にする場合，化合物が血液-脳関門(blood-brain barrier)を通過して脳に到達する必要がある．

以下に，免疫学的手法を用いたプリオン病の予

防・治療法開発について述べる.

## 免疫学的手法を用いたプリオン病の予防・治療法開発

近年，免疫療法，すなわちPrPによる能動免疫や抗PrP抗体を用いた受動免疫などがプリオン病に有用であることを示唆する報告がつぎつぎとなされている.

プリオン感染細胞への抗PrP抗体投与によって$PrP^{Sc}$複製が抑制され，既存の$PrP^{Sc}$が分解・除去されることが示された[9,10]．抗PrP抗体は$PrP^{C}$上のある領域に結合し，$PrP^{Sc}$の複製過程を抑制するらしい.

さらに，プリオンの末梢からの(腹腔内)投与によるプリオン病動物モデルにおいて，PrPによる能動免疫[11]，あるいは抗PrP抗体[12-14]がプリオン病の発症を遅延・抑制することが報告された.

最近の報告[13]では，プリオンの腹腔内投与後，脾における$PrP^{Sc}$の蓄積が最大レベルに達したときにはじめて抗PrP抗体を投与した場合でも抗体投与によって末梢における$PrP^{Sc}$のレベルやプリオンの感染性を顕著に減少させることができること，未治療動物では死亡してしまう300日を過ぎても治療を継続している動物は無症状のままであることなどが報告され，受動免疫療法がきわめて有効である可能性が示唆されている.

また，$PrP^{C}$で能動免疫する場合は$PrP^{C}$は宿主の自己成分であるため，免疫学的寛容ということが問題になる．ダイマー化したPrPを免疫原として投与すると抗体が効率よく産生され，膜表面に存在する$PrP^{C}$と結合し，$PrP^{Sc}$への転換過程を抑制することが報告された[15]．

こうした免疫療法はプリオン病の末梢段階においてのみ有効であり，感染が中枢神経系に波及した段階，あるいは直接脳内にプリオンが接種された場合には無効である．抗PrP抗体は血液-脳関門を通過せず，脳内の$PrP^{Sc}$複製過程には効果を発揮できないものと推測される．これはAlzheimer病動物モデルにおいて脳内に蓄積するアミロイドβ蛋白(Aβ)に対する抗体を末梢から投与することによって脳内のAβ沈着を抑制・除去することができるという観察とは対照的であり，Alzheimer病動物モデルの場合は抗Aβ抗体が末梢のAβを減少させることにより脳からのAβの“ひきぬき”が起こることが推定されている[16]．

また，非特異的な免疫療法として先天免疫(innate immunity)を刺激することが知られているCpGオリゴデオキシヌクレオチドをプリオン腹腔内接種後の動物に投与すると，感染マウスの生存期間を有意に延長することが報告されている[17]．抗プリオン効果のメカニズムは明らかではないが，マクロファージ，単球，樹状突起細胞を刺激し，抗PrP反応を強化している可能性がある[17]．

最近，$PrP^{C}$をヒト免疫グロブリンGのFc部位(Fcγ)へ結合させて可溶性かつダイマー化した$PrP^{C}$($PrP\text{-}Fc_2$)を発現させたマウスにおいて，プリオン接種後，$PrP^{Sc}$の複製・蓄積，プリオン病の発症が遅延することが報告された[18]．このマウスの脳において，$PrP\text{-}Fc_2$はlipid raftにおいて$PrP^{Sc}$と複合体を形成するがプロテアーゼ抵抗性を獲得せず，$PrP\text{-}Fc_2{}^{Sc}$への転換に抵抗性であることが示唆された．$PrP\text{-}Fc_2$を発現するが，内因性$PrP^{C}$をノックアウトしたマウスはプリオン病に抵抗性で$PrP\text{-}Fc_2{}^{Sc}$を蓄積せず，他の動物へプリオン病を伝播させることはなかった．$PrP\text{-}Fc_2$はプリオンの腹腔内接種動物ばかりでなく，プリオンを脳内接種された動物においても有効であった．$PrP\text{-}Fc_2$は$PrP^{Sc}$を隔離して，$PrP^{Sc}$をPrP転換の際の鋳型として使えないようにすることが示唆される．こうした可溶性PrP誘導体はPrP転換過程にアンタゴニストとして作用する新しい種類の予防・治療薬候補であり，今後，トランスジェニックモデル以外での効果や副作用の検討が待たれる.

## おわりに

PrP高次構造を標的としたプリオン病の治療法開発について概説した.

プリオン病の発症過程にはPrPの高次構造転換メカニズム以外にも，まだ多数の不明な点がある．たとえば，プリオン病脳の神経細胞内において，$PrP^{C}$の代謝過程が変化し$PrP^{Sc}$が蓄積して神経細胞死が生じるメカニズムはいまだ十分明らかにされていない．こうした点が解明されることにより，あらたな分子治療の標的が見出されることになろ

う．また，本文中にも述べたように，有用な治療法の開発と同時に，PrP 高次構造を標的とするような高感度の診断法の開発も必須である．研究の進展を期待したい．

## 文献


1) 山田正仁：臨床神経，2003．（印刷中）
2) Prusiner, S. B.：Prion Biology and Diseases. Cold Spring Harbor Laboratory Press, New York, 1999.
3) Mallucci, G. et al.：*Science*, **302**：871-874, 2003.
4) Brown, P.：*Neurology*, **58**：1720-1725, 2002.
5) Forloni, G. et al.：*Proc. Natl. Acad. Sci. USA*, **99**：10849-10854, 2002.
6) Adjou, K. T. et al.：*J. Gen. Virol.*, **84**：2595-2603, 2003.
7) Sigurdsson, E. M. et al.：*J. Biol. Chem.*, **278**：46199-46202, 2003.
8) Korth, C. et al.：*Proc. Natl. Acad. Sci. USA*, **98**：9836-9841, 2001.
9) Peretz, D. et al.：*Nature*, **412**：739-743, 2001.
10) Enari, M. et al.：*Proc. Natl. Acad. Sci. USA*, **98**：9295-9299, 2001.
11) Sigurdsson, E. M. et al.：*Am. J. Pathol.*, **161**：13-17, 2002.
12) Heppner, F. L. et al.：*Science*, **294**：178-182, 2001.
13) White, A. R. et al.：*Nature*, **422**：80-83, 2003.
14) Sigurdsson, E. M. et al.：*Neurosci. Lett.*, **336**：185-187, 2003.
15) Gilch, S. et al.：*J. Biol. Chem.*, **278**：18524-18531, 2003.
16) DeMattos, R. B. et al.：*Proc. Natl. Acad. Sci. USA*, **98**：8850-8855, 2001.
17) Sethi, S. et al.：*Lancet*, **360**：229-230, 2002.
18) Meier, P. et al.：*Cell*, **113**：49-60, 2003.


*　　*　　*

# INFECTIOUS DISEASES REPORT

長崎大学名誉教授　松本　慶蔵　監修

## ▶風疹*1◀

【解説・川崎医科大学 小児科第1講座 助教授　寺田　喜平】

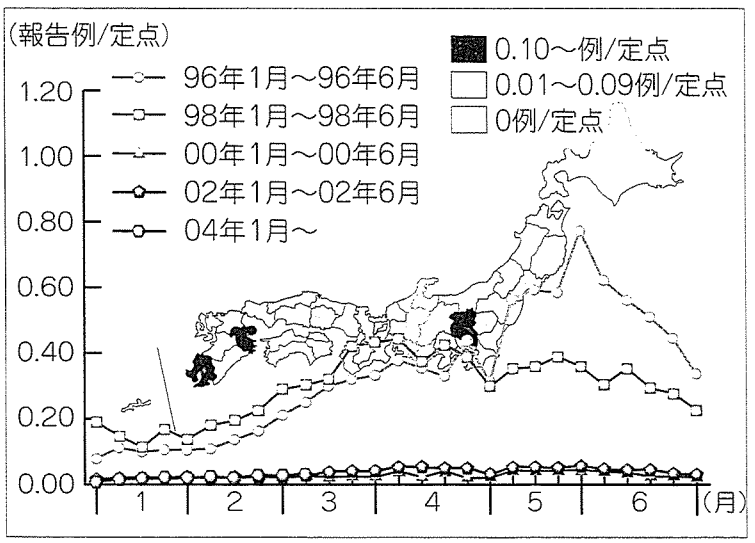


風疹は妊婦が感染すると胎児が先天性風疹症候群（CRS）になることがあり，少子化の中，次世代の子供達を守るために重要な疾患である。1995年予防接種法改正施行後，対象が女子中学生から生後12～90カ月の幼児（男女）となった。そのため，1995年以降定点当たりの報告数が1.2を超えた年はなくなった。しかし，経過措置時の接種率は低く，その頃の中学生は最高23歳になった。わが国では，抗体調査から女性約70万人以上，男性450万人以上が感受性者と推定されている。昨年度全国的な風疹の流行はなかったが，岡山県で散在性小流行があり，CRS２例と不顕性胎児感染２例が発生した。その後，広島県と東京都で各１例のCRSを確認した。流行パターンは，はじめ小流行から1～2年漸増し，ピーク後漸減していった状況を考慮すると，今後数年間流行が予想される。とくに，春先から流行が始まるので，本年は今後の動向に注意する必要がある。

## ▶トピックス◀

### ●クロイツフェルト・ヤコブ病●

【解説・金沢大学大学院医学系研究科 脳病態医学講座 脳老化・神経病態学（神経内科学）教授　山田　正仁】

クロイツフェルト・ヤコブ病（CJD）は世界中で1年間に人口100万人あたり，ほぼ1人の発症率といわれているが，最近，わが国を含め世界各国で増加傾向が報告されている。これは疾患に対する認識が高まったことと関連している可能性もあるが，長期に渡る綿密なサーベイランスが必要である。

厚生労働省難治性疾患克服研究事業『プリオン病および遅発性ウイルス感染に関する調査研究』班・CJDサーベイランス委員会は，わが国のプリオン病について全例実地調査を原則にサーベイランスを行っている。平成11年から15年10月までに登録された440例のプリオン病についてみると，孤発性CJD 343例（78%），遺伝性プリオン病 52例（12%）（内訳：家族性CJD 31例［7%］，ゲルストマン・ストロイスラー・シャインカー病 20例［5%］，致死性家族性不眠症 1例［0.2%］），感染性CJD（すべて硬膜移植後）41例（9%）に分類された。わが国では硬膜移植後のCJDが多いことが特徴であり，世界的な問題となっているウシ海綿状脳症（BSE）に関連する変異型CJDは現在まで１例も確認されていない。

硬膜移植後CJD患者数は増加を続けており，過去の調査で判明した者と本サーベイランスの結果とを加えると合計102例となった。多くの患者は1987年に硬膜の処理法が変更される前に移植を受けた者であり，移植からCJD発症までの潜伏期間の平均は125カ月（約10年），最長は275カ月（約23年）である。潜伏期間は長期化する傾向にあり，今後も硬膜移植後のCJD患者が新たに発症してくることが予想される。

## ▶平成16年10週　第3102表　報告数・定点当り報告数，疾病・都道府県別より*2◀

| | インフルエンザ | | 咽頭結膜熱 | | A群溶血性レンサ球菌咽頭炎 | | 感染性胃腸炎 | | 水　痘 | | 手足口病 | | 伝染性紅斑 | | 突発性発しん | | 百日咳 | |
|---|---|---|---|---|---|---|---|---|---|---|---|---|---|---|---|---|---|---|
| | → | | ⬈ | | ⬈ | | → | | ⇗ | | → | | → | | → | | → | |
| | 報告数 | 定点当り | 報告数 | 定点当り | 報告数 | 定点当り | 報告数 | 定点当り | 報告数 | 定点当り | 報告数 | 定点当り | 報告数 | 定点当り | 報告数 | 定点当り | 報告数 | 定点当り |
| 総数 | 24891 | 5.29 | 556 | 0.18 | 6602 | 2.17 | 30175 | 9.93 | 6566 | 2.16 | 156 | 0.05 | 939 | 0.31 | 1799 | 0.59 | 26 | 0.01 |

（当該週と過去5年間の平均の比〔対数〕を矢印にて表した。→：−0.50～0.50，⇗:平均±1SD，⬈：平均±2SD）

（＊1～2は国立感染症研究所 感染症情報センター「厚生労働省 感染症発生動向調査事業のデータ」をもとに作成）

# 細菌性赤痢

【解説・東京都立北療育医療センター 院長　増田　剛太】

細菌性赤痢は，腸内細菌科に属するグラム陰性桿菌である赤痢菌属（A群：*Shigella dysenteriae*，B群：*S. flexneri*，C群：*S.boydii*，D群：*S. sonnei*の4群に大別）を病原体とし，大腸壁の潰瘍を伴う炎症性病変を主体とする腸管感染症である。臨床症状としては発熱，下腹部痛，テネスムス（しぶり腹）と血便・粘血を混じた頻回の下痢（図1）が挙げられる。赤痢菌感染は患者糞便に汚染された飲食物の摂食により成立する。10～100個の生菌により発病するほど感染力が強く（患者糞便1グラム当たりの赤痢菌数は$10^3$～$10^9$），家族内伝播の発生もまれではない。

細菌性赤痢は感染症法で二類感染症に分類され，他個体へ蔓延させる可能性が高い発症者は入院勧告，措置により感染症指定医療機関への入院対象となる。さらに，病原体がまだ同定されていないが本疾患である可能性が高い有症症例（疑似症例）も同様に扱う。保菌者は入院の対象としない。

現在，世界的に流行している赤痢菌型は弱毒菌である*S. sonnei*であり，その結果，細菌性赤痢全体としての臨床症状は概して軽症であるため（表1），サルモネラやカンピロバクターなどの細菌性，さらにウイルス性腸炎との臨床的鑑別が困難である。

わが国の本疾患症例数は第二次世界大戦後の混乱期に年間10万人を数えたが，国内の衛生環境の改善とともに報告数が減少して1974年以降は1,000人台で経過し（伝染病統計），1999年以後は1,000人以下となった（感染症発生動向調査）。今日のわが国の症例の70～80%は発展途上国からの帰国者に生じた輸入例であるが，感染経路不明の散発・集団例や輸入食品を媒体とした集団発生事例も報告される。

かつて小児に好発した疫痢や菌血症・関節炎を合併症とする症例は，今日では皆無に近い。細菌性赤痢の診断は糞便培養での赤痢菌分離により確定するが，培養は必ず抗菌薬投与開始前に行なう。

細菌性赤痢の治療で重要なのは，①重症度に合わせた食餌制限と②水・電解質溶液（スポーツドリンクなど）の飲用である。5～10回/日程度の下痢症例での食餌は全粥または消化のよい食物の少量摂取とする。重症例では絶食とし，点滴による水分補給を行なう。③抗菌薬投与は臨床症状と排菌期間の短縮に極めて有効である。通常，この目的にニューキノロン薬やホスホマイシンが3～5日間投与される。

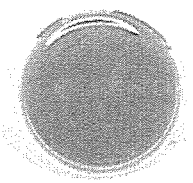

図1　プラスチックコップに採取した細菌性赤痢患者の血性水様便

テネスムスを伴い頻回に排出されるため，一回量は多くない。

表1　細菌性赤痢の臨床像（n=221）

| 症状 | 陽性数（%） |
|---|---|
| 水様便 | 180/210(85.7) |
| 血便 | 53/213(24.9) |
| 発熱≧38℃ | 87/192(45.3) |
| 腹痛 | 144/210(68.6) |
| 嘔気・嘔吐 | 30/212(14.2) |
| 症状持続期間 | 1～≧10日　（中央値5日） |
| 排便回数 | 1～≧21回/日（中央値6回/日） |

東京都立駒込病院　1985～1994年症例．保菌者例・混合感染例を除く
（増田剛太：新内科治療ガイド［矢崎義雄，ほか編集］，pp.1496-1498，文光堂，1999，より）

制作・発行：医薬ジャーナル社
大阪市中央区淡路町3丁目1番5号　淡路町ビル21　〒541-0047　代表 06(6202)7280　FAX 06(6202)5295
東京都千代田区三崎町3丁目1番1号　高橋セーフビル　〒101-0061　代表 03(3265)7681　FAX 03(3265)8369
提　　供：大正富山医薬品株式会社

# 6 孤発性クロイツフェルト・ヤコブ病の嗅上皮における異常プリオン蛋白の検出

Detection of Pathologic Prion Protein in the Olfactory Epithelium in Sporadic Creutzfeldt-Jakob Disease

## CJDの診断における嗅粘膜生検の有用性が示唆された

**【背景・目的】**ヒトの伝播性海綿状脳症あるいはプリオン病の特徴は、宿主の正常型のプリオン蛋白（$PrP^{C}$）が立体構造上の修飾を受け、不溶性でプロテアーゼ抵抗性の異常プリオン蛋白（$PrP^{Sc}$）になることにある。

孤発性クロイツフェルト・ヤコブ病（CJD）は、急速進行性の痴呆、ミオクローヌス、脳波上の周期性同期性放電、脳脊髄液中の14-3-3蛋白上昇などを示し、PrP遺伝子コドン129の多型と$PrP^{Sc}$の性質がその表現型に影響している。しかし、現時点では脳生検以外に生前に確定診断しうる末梢性の診断マーカーは存在しない。

嗅皮質と嗅覚路は孤発性CJDにおいて高率に侵されることが知られており、著者らは嗅粘膜を含む嗅覚路の末梢領域を検索して$PrP^{Sc}$の鼻腔上皮における沈着について評価した。

**【方法】**神経病理学的に確定診断された9例の孤発性CJDを対象とした。

剖検時に脳、嗅粘膜の付着した篩板（図）、および周辺の呼吸上皮を採取した。対照として神経疾患のない5例とそのほかの神経疾患患者（アルツハイマー病など）を含めた。嗅粘膜、呼吸粘膜、頭蓋内嗅覚系（嗅球、嗅索、梨状葉前皮質、内嗅領皮質）について、病理、免疫組織化学的検索用標本、ウエスタンブロット法用の凍結標本を採取した。PrPの免疫組織化学的検索は3F4抗体（抗PrPモノクローナル抗体）を用いABC法で行った。ウエスタンブロットは組織100mgを用い、プロテイナーゼK処理後にサンプルを電気泳動してブロットした後、3F4抗体に反応させた。

**【結果】**孤発性CJD 9例の臨床症状、脳波所見、髄液14-3-3蛋白、コドン129多型、$PrP^{Sc}$のタイプを表に示す。PrP遺伝子変異を有する症例はなかった。

CJDの嗅上皮細胞は組織学的には明らかな異常所見を示さなかった。しかし、PrP免疫染色では対照例はすべての組織が陰性であったが、CJDは全例において嗅受容細胞の嗅毛に強い陽性所見を、嗅上皮基底細胞には弱い陽性所見を認めた。呼吸上皮は陰性であった。CJDの嗅球、嗅索、嗅皮質にはPrPの沈着が認められた。

ウエスタンブロット法で嗅上皮および呼吸上皮における$PrP^{C}$発現をみると、それぞれ、脳の約20％、13％の量の発現がみられた。プロテイナーゼK処理後の$PrP^{Sc}$をリン酸タングステン酸塩を用いて沈降させて検討すると、嗅上皮にのみ$PrP^{Sc}$が見いだされ、糖鎖がついていないPrP断片のサイズは、コドン129がMet/Metの全例で22kD、Val/Valの症例9では21kDであった。孤発性CJDの呼吸上皮や対照例の組織では$PrP^{Sc}$は検出されなかった。

嗅覚領域、新皮質、皮質下灰白質、小脳における$PrP^{Sc}$の分布をみると、コドン129がMet/Metのケースでは、新皮質に大量、視床や基底核や小脳では比較的少量、海馬では極少量であったが、一方で内嗅領皮質や嗅皮質では比較的大量の$PrP^{Sc}$を認めた。嗅球や嗅索などの領域にも$PrP^{Sc}$が検出された。

**図●末梢嗅覚系**

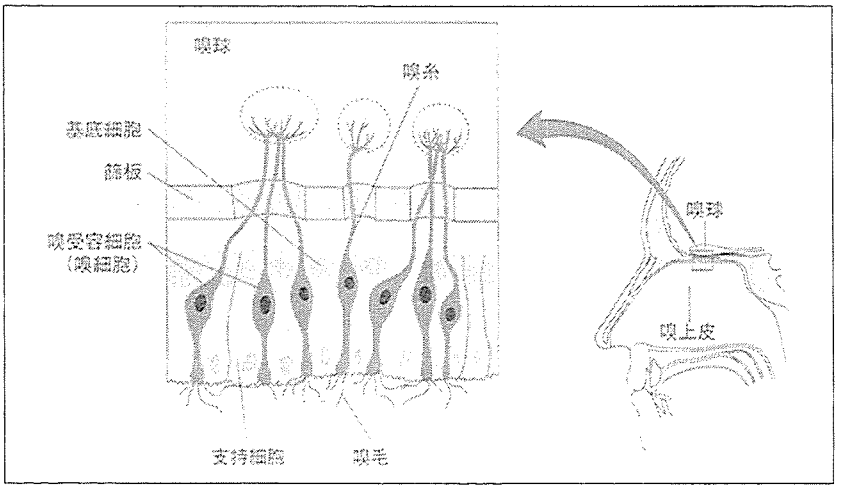


嗅受容細胞（嗅細胞）の樹状突起の先端部には嗅毛が数本あり、嗅毛にはにおい受容部位がある。嗅受容細胞は嗅糸とよばれる一本の細い軸索を篩板を貫いて嗅球へ送っている。嗅上皮は3種類の細胞からなり、嗅受容細胞以外に支持細胞、基底細胞がある。

Zanusso G, Ferrari S, Cardone F et al
*N Engl J Med* 348: 711～719, 2003

コドン129がVal/Valである症例9においては、$PrP^{Sc}$は新皮質では少量であったが、小脳や皮質下灰白質では大量に認められ、嗅球、嗅索、嗅皮質では中等量が認められた。

【考察】本研究により孤発性CJDでは嗅覚路が侵され、$PrP^{Sc}$が嗅粘膜の神経上皮に検出されることが示された。嗅粘膜生検の診断的意義が問題となるが、本研究は剖検組織を用いたものであるので、孤発性CJDの臨床経過のどの段階で嗅粘膜に$PrP^{Sc}$が出現するかは不明である。嗅覚障害を初発症状としている症例もあることから初期から嗅覚系が侵されている可能性もあり、嗅粘膜生検が孤発性CJDの初期診断上で有用な方法となる可能性がある。

また、嗅粘膜が感染源となって嗅覚経路がプリオンの感染経路になる可能性もあり、鼻腔上部を含む内視鏡検査や外科手術では十分感染に注意する必要がある。嗅上皮における$PrP^{Sc}$蓄積は、嗅上皮がプリオン感染ルートの入口に位置することを示唆するのか、あるいは単に神経系におけるプリオン感染が拡がった結果であるのかなどの問題は今後の課題である。

【結論】孤発性CJDの嗅粘膜の神経上皮において$PrP^{Sc}$が沈着していることが示された。嗅粘膜生検は診断上有用である可能性がある。また、嗅覚経路による感染はプリオン伝播の一形式である可能性がある。

山田正仁［金沢大学大学院医学系研究科脳老化・神経病態学（神経内科学）教授］

表●孤発性CJD9例の特徴（全例とも髄液14-3-3蛋白陽性）

| 症例番号 | 発症年齢 | コドン129 | $PrP^{Sc}$ | 初発症状 | 期間 | 臨床経過 | 脳波 |
|---|---|---|---|---|---|---|---|
| 1 | 72歳（男性） | Met/Met | 21 | 幻覚 | 5カ月 | 失調、ミオクローヌス | PSWs |
| 2 | 71歳（女性） | Met/Met | 21 | 幻覚 | 8カ月 | 痴呆、失調、ミオクローヌス | PSWs |
| 3 | 73歳（女性） | Met/Met | 21 | 失調、構音障害 | 16カ月 | 痴呆 | PSWs |
| 4 | 74歳（女性） | Met/Met | 21 | 痴呆 | 2カ月 | 失調 | PSWs |
| 5 | 69歳（女性） | Met/Met | 21 | 皮質盲 | 5カ月 | 痴呆、ミオクローヌス | DS |
| 6 | 59歳（男性） | Met/Met | 21 | 痴呆 | 3カ月 | ミオクローヌス | PSWs |
| 7 | 55歳（女性） | Met/Met | 21 | 嗅覚障害 | 5カ月 | 痴呆 | PSWs |
| 8 | 52歳（男性） | Met/Met | 21 | 痴呆 | 3カ月 | 失調、ミオクローヌス | PSWs |
| 9 | 64歳（女性） | Val/Val | 19 | 失調 | 5カ月 | 痴呆 | DS |

＊糖鎖のついていないプロテイナーゼK抵抗性$PrP^{Sc}$断片の分子量
PSWs：周期性鋭徐波複合
DS：びまん性徐波化

## REMARK

### CJDの新規診断法の開発

山田正仁

プリオン病の確定診断は異常プリオン蛋白$PrP^{Sc}$の検出による。最近、採取が容易な末梢組織や体液を用いて異常PrPを検出し、脳生検なしに異常PrP蓄積を診断しようとする試みがなされている。たとえば、高感度の検出法を用いて患者の髄液から$PrP^{Sc}$を検出できたとする報告（Bieschke J et al: *Proc Natl Acad Sci USA* 97: 5468～5473, 2000）、患者の尿中にプロテアーゼ抵抗性PrPが検出されるとする報告（Shaked GM et al: *J Biol Chem* 276: 31479～31482, 2001）などがあり、臨床応用への可能性が検討されている。また、変異型CJDでは扁桃組織に$PrP^{Sc}$の沈着がみられることから、扁桃生検が診断上有用である。

本研究では孤発性CJD患者の嗅上皮に$PrP^{Sc}$が見いだされ、嗅粘膜生検が診断上有用である可能性が示唆された。ただし、本研究は剖検時の組織を用いた研究であるため、いくつかの問題がある。たとえば、臨床経過のどの段階から嗅上皮に$PrP^{Sc}$が検出されるようになるのかが不明である。また、免疫組織化学のみならずウエスタンブロット法で$PrP^{Sc}$を正確に検出するためには、ある程度以上の量の嗅粘膜組織を生検で採取する必要があろう。しかし、嗅粘膜生検は有用な診断手段になる可能性があり、孤発性CJDの病型別（MM1/MM2/MV1/MV2/VV1/VV2）やほかのプリオン病についても詳細な検討を加える必要がある。

また、嗅粘膜が感染源となって嗅覚系がプリオンの感染経路になる可能性が指摘されているが、この点も臨床上の大きな問題である。鼻腔上部を含む内視鏡検査や外科手術は医原性感染をおこす可能性があることに十分注意する必要があろう。

# 質疑応答 Q&A

◎質問は「日本医事新報社質疑応答係」宛にはがき、封書、FAX（〇三―三二九二―一五五〇）でお願いします。
◎質問は読者の方々がご覧になるための誌上掲載が前提です。
◎誌上匿名の取り扱いを致しますが、連絡の必要がありますので、住所・氏名・電話番号を必ず明記してください。
◎質問の採否は編集部にご一任ください。
◎質問は無料ですが、誌上掲載前に回答をご覧になりたい場合は、一件につき送付手数料一〇〇〇円を切手同封か、現金書留等を利用してお送りください。

## 一般診断

### 虚血性心疾患の聴診におけるⅠ音の減弱

**Q** 一、虚血性心疾患の時、聴診上、Ⅰ音は心臓の強さを表し、特に心筋が傷害された場合、膜式では聴こえが悪く、ベル式で聴こえるといわれる。例えば糖尿病の場合、無痛性心筋梗塞が生じていると解釈できるか（心不全以外の時でギャロップ以外）。

二、また、心聴診所見がdistantであるといわれるが、その意義について、実地医家向けに解説を。

以上、さわやまクリニック・沢山俊民院長に。（群馬県　N）

**A** 一、Ⅰ音の強さ（大きさ）には音量と亢進度が関係している。Ⅰ音の強さは他の条件（とりわけ心電図PR間隔の長短）が一定ならば心筋の収縮性の強弱（左室心筋の収縮速度）に関連する。例えば、甲状腺機能亢進患者や若年健常者を聴診すると、Ⅰ音が亢進していることに気づくであろう。

一方、Ⅰ音がベル式では聴きやすいが膜式で聴きにくいという所見は「Ⅰ音の減弱」と表現され、心筋収縮性の低下を意味するが、疾患特異性はない。しかし、もし正常大であったⅠ音が、心筋梗塞後に減弱したことがわかれば、それは梗塞により心筋収縮性が減弱したためといえよう。

二、次に、「聴診所見がdistantである」という表現は、心血管系そのものの異常によるためというよりも、心臓と胸壁との距離が遠い（distant）状態で、代表は肥満例と肺気腫例である。これらの場合には二心音とも聴き取りにくく（ただ音量が小さい）、呼吸音も当然distantである。

図1に、正常心音、Ⅰ音減弱ならびにdistant心音をそれぞれ示しておく。

図1　心尖部における3状態の心音図所見[1]

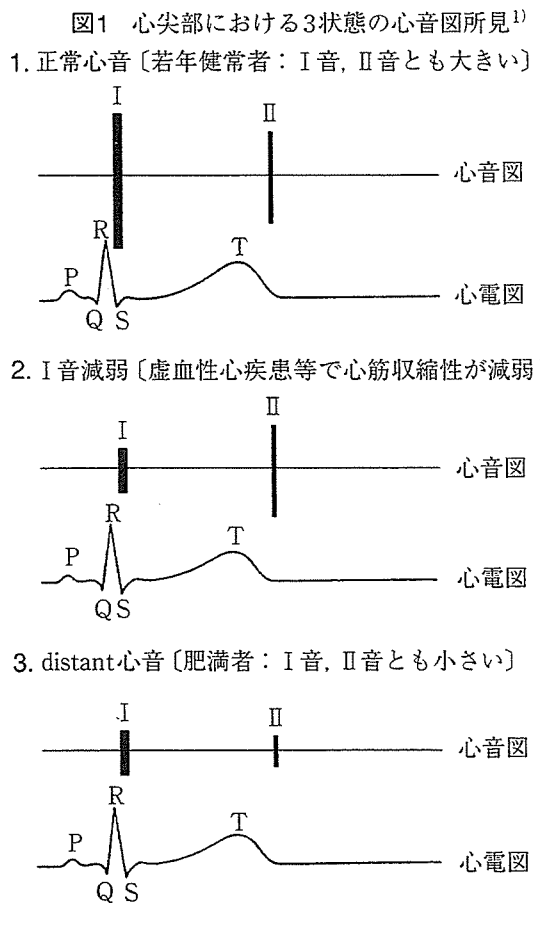


〔文　献〕

1）沢山俊民：CDによる聴診トレーニング　心音編・改訂第2版，南江堂，1994，p17.

（さわやまクリニック　倉敷心臓病予防施設　沢山俊民）

## 内　科

### BSE病原体に対する感受性の人種差

**Q** 日本人の多くがウシ海綿状脳症（BSE）と同じ病原に感染する遺伝子型を持っており、欧米人よりむしろBSEの病原体に感染しやすいと聞いたが、その理由について。（鳥取県　E）

**A** ウシのBSEやヒトのクロイツフェルト・ヤコブ病（CJD）などの一群の疾患は、種を越えて感染する人畜共通感染症であり、感染因子として、ウイルスなどの通常の病原体とは異なるプリオンが提唱され、現在これらはプリオン病と総称されている。

ヒトのプリオン病はその病因から、①何の発病の背景も見出されない特発性（孤発性CJD）、②感染

性、③遺伝性に大別される。近年、感染性プリオン病の一つとして、ウシのBSEから伝播したとされる変異型と呼ばれる新しいタイプのCJD（変異型CJD，variant CJD；vCJD）が英国を中心に発生し、わが国でもBSEのウシが認定されたことから、大きな社会問題となっている。わが国におけるサーベイランスでは、現在までにvCJDと認定された患者はおらず、感染性プリオン病はすべて屍体由来の硬膜移植後のCJDである。

プリオンの主要構成成分であるプリオン蛋白（PrP）は、宿主の第20染色体短腕上の遺伝子（PrP遺伝子）によってコードされており、主に中枢神経系に、少量ではリンパ系組織などに発現している。正常のPrPはプロテアーゼ感受性で、感染性はない（正常型$PrP^C$）。一方、感染性のPrP（感染型PrP：$PrP^{Sc}$）はプロテアーゼ抵抗性のコアを有し、$PrP^C$が翻訳後に立体構造の変化を起こし、作り出される。プリオン病では、$PrP^{Sc}$の蓄積あるいは正常の$PrP^C$機能の消失により、ニューロンやシナプスの障害が生ずると考えられている。

PrP遺伝子には多数の変異、多型の部位が存在する。変異は遺伝性プリオン病の病因となり、一方、多型は孤発性CJDや感染性プリオン病の疾患感受性（発病しやすさ）や表現型（病像）に影響する。

PrP遺伝子に見出されている多型の中で、コドン129の多型は最も一般的にみられ、vCJDの感受性にも関係している。コドン129多型にはメチオニン（M）とバリン（V）の二種類のアリル、MM、MV、VVの三種類の遺伝子型がある。コーカサス人種（英国）におけるM／Vのアリル頻度は〇・六二五／〇・三七五であるのに対し、日本人では〇・九五八／〇・〇四二であり、アリル頻度に明らかな人種差がある[1,2]。

コーカサス人種において、孤発性CJDではコドン129がホモ接合体（MMあるいはVV）である頻度（八七～九五％）が健常者のそれ（ほぼ五〇％）と比べて有意に高く、ホモ接合体を有することが孤発性CJDのリスクであると考えられている[1]。しかし、もともとMMのホモ接合体が九〇％以上を占める日本人では、この関連は容易には検証されえない[2]。また、屍体由来の下垂体由来成長ホルモン製剤の使用や硬膜移植等によって感染した医原性CJDにおいても、同様にホモ接合体の頻度が高い[3]。

注目すべきは、コドン129がMMのホモ接合体であることが、変異型CJD発症のリスクと考えられている点である。英国でこれまでに検索されたvCJD一一三例のすべて（一〇〇％）がMMのホモ接合体であった[4]。一方、英国の一般人口におけるMMの頻度は三七％にすぎない[1]。前述したように、日本人では、MMのホモ接合体を有する人が全体の九〇％以上を占めている[2]。したがって、英国におけるvCJDとMMホモ接合体の関連が日本人にそのまま当てはまるものと仮定し、さらに、日本人が英国と同程度にBSE因子に曝露されたと仮定した場合、日本人は英国人よりもvCJDを発症しやすいものと推定される。

最近、vCJDを後になって発症したドナーから輸血を受けた英国人患者が五年後に非神経疾患で死亡し、剖検したところ、脳には異常PrP蓄積はなかったものの、脾臓に異常PrPの蓄積を認めた[5]。興味深いことには、発症前であったと考えられるこの患者のPrP遺伝子コドン129多型はMVのヘテロ接合体であった[5]。

これらのことから、英国で人口の約五〇％を占めるMVを有するサブグループは、BSEからの直接感染あるいは輸血による二次感染に曝露された後、MMホモ接合体とは異なる非常に長い潜伏期間を経て発症してくる可能性があること、これらの発症前の患者が献血などによって医原性感染を起こす危険性があることなどの問題が提起されている。

〔文　献〕


1) Palmer MS, Dryden AJ, Hughes T, et al：Nature 352：340, 1991.
2) Doh-ura K, Kitamoto T, Sakaki Y, et al：Nature 353：801, 1991.
3) Brown P, Preece M, Brandel J-P, et al：Neurology 55：1075, 2000.
4) The UK National Creutzfeldt-Jakob Disease Surveillance Unit. http://www.cjd.ed.ac.uk/eleventh/rep2002.htm
5) Peden AH, Head MW, Ritchie D, et al：Lancet 364：527, 2004.


（金沢大大学院 脳老化・神経病態学教授　山田正仁）

Available online at www.sciencedirect.com

SCIENCE DIRECT

Brain Research 1038 (2005) 208–215

BRAIN RESEARCH

www.elsevier.com/locate/brainres

Research report

# Brain pericytes contribute to the induction and up-regulation of blood–brain barrier functions through transforming growth factor-β production

Shinya Dohgu[a], Fuyuko Takata[a], Atsushi Yamauchi[a], Shinsuke Nakagawa[b], Takashi Egawa[a], Mikihiko Naito[c], Takashi Tsuruo[c], Yasufumi Sawada[d], Masami Niwa[b], Yasufumi Kataoka[a,*]

[a]*Department of Pharmaceutical Care and Health Sciences, Faculty of Pharmaceutical Sciences, Fukuoka University, 8-19-1 Nanakuma, Jonan-ku, Fukuoka 814-0180, Japan*

[b]*Department of Pharmacology 1, Graduate School of Medicine, Nagasaki University, 1-12-4 Sakamoto, Nagasaki 852-8523, Japan*

[c]*Institute of Molecular and Cellular Biosciences, University of Tokyo, Bunkyo-ku, Tokyo 113-0032, Japan*

[d]*Department of Medico-Pharmaceutical Sciences, Graduate School of Pharmaceutical Sciences, Kyushu University, 3-1-1 Maidashi, Higashi-ku, Fukuoka 812-8582, Japan*

Accepted 10 January 2005

**Abstract**

The blood–brain barrier (BBB) is a highly organized multicellular complex consisting of an endothelium, brain pericytes and astrocytes. The present study was aimed at evaluating the role of brain pericytes in the induction and maintenance of BBB functions and involvement of transforming growth factor-β (TGF-β) in the functional properties of pericytes. We used an in vitro BBB model established by coculturing immortalized mouse brain capillary endothelial (MBEC4) cells with a primary culture of rat brain pericytes. The coculture with rat pericytes significantly decreased the permeability to sodium fluorescein and the accumulation of rhodamine 123 in MBEC4 cells, suggesting that brain pericytes induce and up-regulate the BBB functions. Rat brain pericytes expressed TGF-β1 mRNA. The pericyte-induced enhancement of BBB functions was significantly inhibited when cells were treated with anti-TGF-β1 antibody (10 μg/ml) or a TGF-β type I receptor antagonist (SB431542) (10 μM) for 12 h. In MBEC4 monolayers, a 12 h exposure to TGF-β1 (1 ng/ml) significantly facilitated the BBB functions, this facilitation being blocked by SB431542. These findings suggest that brain pericytes contribute to the up-regulation of BBB functions through continuous TGF-β production.


*Theme:* Cellular and molecular biology
*Topic:* Blood–brain barrier

*Keywords:* Blood–brain barrier; Pericyte; Transforming growth factor-β; P-glycoprotein; Permeability; Mouse brain endothelial cell

## 1. Introduction

The blood–brain barrier (BBB) is highly restrictive of the transport of substances between blood and the central nervous system. The BBB is a complex system of different cellular components including brain microvascular endothelial cells, pericytes and astrocytes. Astrocytes induce and maintain the properties of the BBB including the integration of tight junctions and expression of P-glycoprotein (P-gp) through cell-to-cell contact and the secretion of soluble factors [23]. Brain pericytes are important for control of the growth and migration of endothelial cells and the integrity of microvascular capillaries [22]. Such functions are known to be mediated by transforming growth factor-β (TGF-β) [1,21,25], vascular endothelial growth factor (VEGF)

* Corresponding author. Fax: +81 92 862 2696.
*E-mail address:* ykataoka@cis.fukuoka-u.ac.jp (Y. Kataoka).

0006-8993/$ - see front matter © 2005 Elsevier B.V. All rights reserved.
doi:10.1016/j.brainres.2005.01.027

[14,17] and direct cell-to-cell communications. Pericytes have several apparatuses to directly make contact with endothelial cells: gap junctions, adhesion plaques and peg-and-socket junctions [24]. Soluble factors including TGF-β, VEGF and basic fibroblast growth factor (bFGF) were produced by and released from pericytes [2,24]. These growth factors control the permeability of the BBB [8,26,31]. These evidences indicate that pericytes regulate the brain's endothelial barrier by collaborating with astrocytes.

TGF-β, a family of multifunctional peptide growth factors, has several isoforms (TGF-β1, 2, 3, 4 and 5), shares the same structure (65–80% homology) and displays similar biological activity in vitro [11]. TGF-β acts on two highly conserved single transmembrane receptors with an intracellular serine/threonine kinase domain (TGF-β type I and type II receptors) to activate an intracellular signaling system, such as Smad proteins or the p38 mitogen-activated protein kinase (MAPK) and the extracellular signal-regulated kinase pathway [6]. TGF-β is listed as a potent endogenous substance protecting against neurodegenerative diseases of the central nervous system [11].

Recently, brain pericytes were reported to induce occludin and multidrug resistance-associated protein (MRP) 6 mRNA expression in brain endothelial cells [3,15]. As for BBB functions, brain pericytes reduce the endothelial permeability of the brain [13]. However, little is known about the mechanism behind the facilitatory role of brain pericytes in the induction and maintenance of BBB functions. The aim of this study was to clarify whether TGF-β participates in the pericyte-induced regulation of BBB functions. We made an in vitro model of the BBB by coculturing immortalized mouse brain capillary endothelial (MBEC4) cells with rat brain pericytes. MBEC4 cells are known to have the highly specialized characteristics of brain microvascular endothelial cells including the expression of P-gp [28,29]. BBB functions were assessed based on the permeability coefficient of sodium fluorescein (Na-F) and the cellular accumulation of rhodamine 123 in MBEC4 cells as the paracellular permeability of brain endothelial cells and the functional activity of P-gp, respectively.

## 2. Materials and methods

### 2.1. Animals

Wistar rats aged 2 weeks old were housed in a room at a temperature of 22 ± 2 °C under a 12-h light/dark schedule (lights on at 7:00 h) and given water and food ad libitum. All the procedures involving experimental animals adhered to the law (No. 105) and notification (No.6) of the Japanese Government and were approved by the Laboratory Animal Care and Use Committee of Fukuoka University.

### 2.2. MBEC4 cell culture

MBEC4 cells, which were isolated from BALB/c mouse brain cortices and immortalized by SV40-transformation [28], were cultured in Dulbecco's modified Eagle's medium (DMEM; Invitrogen, Carlsbad, CA, USA) supplemented with 10% fetal bovine serum (FBS), 100 units/ml penicillin and 100 μg/ml streptomycin at 37 °C with a humidified atmosphere of 5% $CO_2$/95% air. They were seeded on 12-well Transwell®-Clear inserts (Costar, MA) and 24-well culture plates (BD FALCON™, BD Biosciences, NJ) at a density of 42,000 cells/insert and 21,000 cells/well, respectively.

### 2.3. Primary culture of rat pericytes

Rat cerebral pericytes were isolated according to the method of Hayashi et al. [13]. Pure cultures of rat cerebral pericytes were obtained by prolonged culture of isolated brain microvessel fragments under selective culture conditions because microvessel fragments contain 23% pericytes [27]. The cerebral cortices from 2-week-old Wistar rats were cleaned of meninges and minced. The homogenate was digested with collagenase CLS2 (1 mg/ml; Worthington, Lakewood, NJ) and DNase I (37.5 μg/ml; Sigma, St. Louis, MO) in DMEM (Sigma) containing 100 units/ml penicillin, 100 μg/ml streptomycin, 50 mg/ml gentamicin and 2 mM glutamine at 37 °C for 1.5 h. Neurons and glial cells were removed by centrifugation in 20% bovine serum albumin (BSA)-DMEM (1000 × $g$ for 20 min). The microvessels obtained in the pellet were further digested with collagenase/dispase (1 mg/ml; Roche, Mannheim, Germany) and DNase I (16.7 μg/ml) in DMEM at 37 °C for 1 h. Microvessel endothelial cell clusters were separated by 33% Percoll (Amersham Biosciences, Piscataway, NJ) gradient centrifugation (1000 × $g$ for 10 min). The obtained microvessel fragments were washed twice in DMEM (first 1000 × $g$ for 8 min, then, 700 × $g$ for 5 min) and placed in uncoated culture flasks in DMEM supplemented with 10% FBS, 100 units/ml penicillin and 100 μg/ml streptomycin at 37 °C with a humidified atmosphere of 5% $CO_2$/95% air. After 14 days in culture, rat pericytes overgrew brain endothelial cells and reached typically 80–90% confluency. The cells were used at passages 2–3.

### 2.4. Preparation of three in vitro BBB models

The preparation of the in vitro BBB models was previously described [7]. In brief, rat pericytes (40,000 cells/cm$^2$) were first cultured on the outside of the collagen-coated polyester membrane (1.0 cm$^2$, 0.4 μm pore size) of a Transwell®-Clear insert (12-well type, Costar) directed upside down in the well. Two days later, MBEC4 cells (42,000 cells/cm$^2$) were seeded on the inside of the insert placed in the well of a 12-well culture plate (Costar) (the

opposite coculture system). In the other (bottom coculture) system, rat pericytes (20,000 cells/cm$^2$) were first cultured in the wells of the 12-well culture plate. After 2 days, MBEC4 cells were seeded on the inside of a Transwell®-Clear insert placed in the plate containing layers of rat pericytes. A monolayer system was also made with MBEC4 cells alone (MBEC4 monolayer).

### 2.5. Paracellular transport of Na-F

To initiate the transport experiments, the medium was removed and MBEC4 cells were washed three times with Krebs–Ringer buffer (118 mM NaCl, 4.7 mM KCl, 1.3 mM $CaCl_2$, 1.2 mM $MgCl_2$, 1.0 mM $NaH_2PO_4$, 25 mM $NaHCO_3$ and 11 mM D-glucose, pH 7.4). Krebs–Ringer buffer (1.5 ml) was added to the outside of the insert (abluminal side). Krebs–Ringer buffer (0.5 ml) containing 100 μg/ml of Na-F (MW 376) (Sigma) was loaded on the luminal side of the insert. Samples (0.5 ml) were removed from the abluminal chamber at 30, 60, 90 and 120 min and immediately replaced with fresh Krebs–Ringer buffer. Aliquots (5 μl) of the abluminal medium were mixed with 200 μl of Krebs–Ringer buffer and then the concentration of Na-F was determined with a CytoFluor Series 4000 fluorescence multiwell plate reader (PerSeptive Biosystems, Framingham, MA) using a fluorescein filter pair (Ex($\lambda$) 485 ± 10 nm; Em($\lambda$) 530 ± 12.5 nm). The permeability coefficient and clearance were calculated according to the method described by Dehouck et al. [5]. Clearance was expressed as microliters (μl) of tracer diffusing from the luminal to abluminal chamber and was calculated from the initial concentration of tracer in the luminal chamber and final concentration in the abluminal chamber: Clearance (μl) = $[C]_A \times V_A / [C]_L$, where $[C]_L$ is the initial luminal tracer concentration, $[C]_A$ is the abluminal tracer concentration and $V_A$ is the volume of the abluminal chamber. During a 120-min period of the experiment, the clearance volume increased linearly with time. The average volume cleared was plotted versus time, and the slope was estimated by linear regression analysis. The slope of clearance curves for the MBEC4 monolayer or coculture systems was denoted by $PS_{app}$, where PS is the permeability-surface area product (in μl/min). The slope of the clearance curve with a control membrane was denoted by $PS_{membrane}$. In the rat pericyte opposite coculture system, the control membrane is the rat pericyte-layered membrane. The real PS value for the MBEC4 monolayer and the coculture system ($PS_{trans}$) was calculated from $1/PS_{app} = 1/PS_{membrane} + 1/PS_{trans}$. The $PS_{trans}$ values were divided by the surface area of the Transwell inserts to generate the permeability coefficient ($P_{trans}$, in cm/min).

### 2.6. Functional activity of P-gp

The functional activity of P-gp was determined by measuring the cellular accumulation of rhodamine 123 (Sigma) according to the method of Fontaine et al. [12]. MBEC4 cells were washed three times with assay buffer (143 mM NaCl, 4.7 mM KCl, 1.3 mM $CaCl_2$, 1.2 mM $MgCl_2$, 1.0 mM $NaH_2PO_4$, 10 mM HEPES and 11 mM D-glucose, pH 7.4). In rat pericyte coculture systems, rat pericytes on the outside of the membrane were removed with a cell scraper. MBEC4 cells were incubated with 0.5 ml of assay buffer containing 5 μM of rhodamine 123 for 60 min. Then, the solution was removed and the cells were washed three times with ice-cold phosphate-buffered saline and solubilized in 1 M NaOH (0.2 ml). Aliquots (5 μl) of the cell solution were removed for measurement of cellular protein according to the method of Bradford [4] using a Bio-Rad protein assay kit (Bio-Rad Laboratories, Hercules, CA). The remaining solution was neutralized with 1 M HCl and the rhodamine 123 content was determined with a CytoFluor Series 4000 fluorescence multiwell plate reader (PerSeptive Biosystems) using a fluorescein filter pair (Ex($\lambda$) 485 ± 10 nm; Em($\lambda$) 530 ± 12.5 nm).

### 2.7. Detection of TGF-β1 mRNA

Total RNA from rat pericytes was extracted using TRIzol™ reagent (Invitrogen). The primer pair used in the reverse transcription-polymerase chain reaction (RT-PCR) was designed based on the nucleotide sequence of the rat TGF-β1 and rat GAPDH. The sequences of primers were as follows: the upper primer 5′-ATACGCCTGAGTGGCTGTCT-3′ and the lower primer 5′-TGGGACTGATCCCATTGATT-3′ for TGF-β1; the upper primer 5′-CTACCCACGGCAAGTTCAAT-3′ and the lower primer 5′-GGATGCAGGGATGATGTTCT-3′ for GAPDH. The expected sizes of the RT-PCR products, predicted from the positions of the primers, were 153 bp for TGF-β1 and 479 bp for GAPDH. A SuperScript One-Step RT-PCR system (Invitrogen) was used for reverse transcription of RNA, and TGF-β1 cDNA was amplified by PCR. Amplification was performed in a DNA thermal cycler (PC707; ASTEC, Fukuoka, Japan) according to the following protocol: cDNA synthesis for 30 min at 50 °C, pre-denaturation for 5 min at 94 °C; 25 cycles of denaturation for 30 s at 94 °C, primer annealing for 30 s at 57 °C and polymerization for 30 s at 72 °C; and a final extension for 5 min at 72 °C. Each 10 μl of PCR product was analyzed by electrophoresis on a 3% agarose (Sigma) gel with ethidium bromide staining. The gels were visualized on a UV light transilluminator and photographed using a DC290 Zoom digital camera (Kodak, Rochester, New York).

### 2.8. Effects of the modulation of TGF-β1 signaling on BBB functions

A TGF-β type I receptor antagonist, SB431542 (TOCRIS, Bristol, UK), and human TGF-β1 (Sigma) were first dissolved in dimethylsulfoxide (DMSO) and 4 mM HCl

containing 1 mg/ml BSA, respectively. They were diluted with serum-free culture medium (0.1% as the final DMSO concentration). MBEC4 cells were cultured for 3 days in the three in vitro BBB models. The inserts and wells were washed three times with serum-free medium prior to the experiments. To examine the influence of the inhibition of TGF-β1 signaling on the pericyte-induced changes in BBB functions, SB431542 (10 μM) and monoclonal anti-human TGF-β1 antibody (10 μg/ml; R&D Systems, Minneapolis, MN) were loaded in both compartments of the opposite coculture system. In the MBEC4 monolayer, cells were exposed to 1 ng/ml TGF-β1 injected into the inside (luminal) or outside (abluminal) of the insert for 12 h and subjected to experiments to test whether MBEC4 cells exhibit functional polarity in response to TGF-β1. TGF-β1 and the TGF-β1 receptor antagonist (SB431542) were applied for 12 h to the inside of the insert in the MBEC4 monolayer to investigate the effect of SB431542 on the TGF-β1-induced changes in BBB functions. In all experiments, controls were performed by treating cells with serum-free medium containing the corresponding amount of DMSO and/or 4 mM HCl containing 1 mg/ml BSA as the vehicle.

### 2.9. Statistical analysis

Values are expressed as the mean ± SEM. Statistical analysis was performed using Student's *t* test. One-way and two-way analyses of variance (ANOVAs) followed by Tukey–Kramer's tests were applied to multiple comparisons. The differences between means were considered to be significant when *P* values were less than 0.05.

## 3. Results

### 3.1. BBB functions in three in vitro BBB models and expression of TGF-β1 mRNA in rat pericytes

After MBEC4 cells were cultured for 3 days, the basal permeability and P-gp efflux pump of MBEC4 cells were evaluated in three models of the BBB (Fig. 1). The permeability coefficient of Na-F for MBEC4 cells significantly decreased by 34.8% and 16.0% in the opposite and bottom coculture systems, respectively, when compared to that in the MBEC4 monolayer (Fig. 1A). The accumulation of rhodamine 123 in MBEC4 cells significantly decreased by 17.8 and 7.8% in the opposite and bottom coculture models relative to the MBEC4 monolayer, respectively (Fig. 1B).

To obtain molecular evidence for the expression of TGF-β1 in rat pericytes, RT-PCR was carried out with a primer pair specific for rat TGF-β1 (Fig. 2). RT-PCR with mRNA obtained from rat pericytes yielded a single product. The size of this product was the same as that expected from the primer positions in rat TGF-β1.

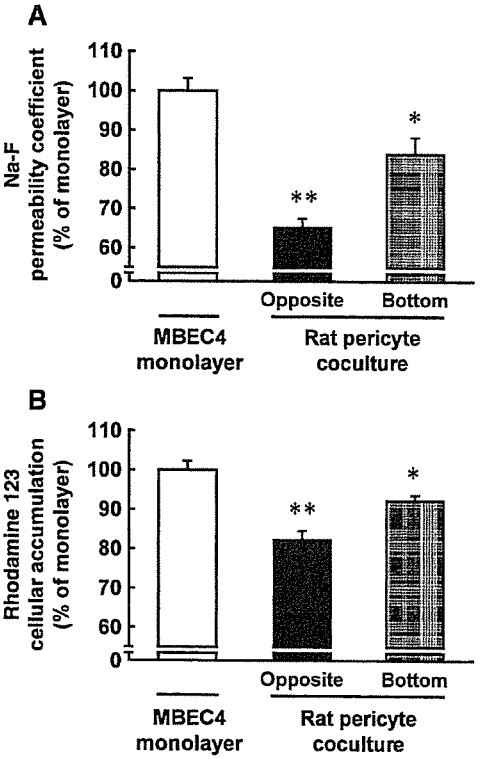


Fig. 1. Permeability and P-gp function of MBEC4 cells in the MBEC4 monolayer and rat pericyte opposite or bottom coculture systems. (A) MBEC4 permeability coefficients of Na-F. Results are expressed relative (%) to the value for the MBEC4 monolayer ($2.7 \pm 0.20 \times 10^{-4}$ cm/min). Values are the means ± SEM ($n$ = 4–12). *$P$ < 0.05, **$P$ < 0.01, significant difference from MBEC4 monolayer. (B) Rhodamine 123 accumulation in MBEC4 cells. Results are expressed relative (%) to the value for the MBEC4 monolayer (1.61 ± 0.25 nmol/mg protein). Values are the mean ± SEM ($n$ = 4–12). **$P$ < 0.01, significant difference from MBEC4 monolayer.

### 3.2. Effect of the inhibition of TGF-β1 signaling on BBB functions in the MBEC4 monolayer and rat pericyte opposite coculture

As shown in Fig. 3, exposure to anti-TGF-β1 antibody for 12 h inhibited the pericyte-induced enhancement of endothelial barrier and P-gp function in rat pericyte cocultures, whereas anti-TGF-β1 antibody had no significant effect on BBB functions in the MBEC4 monolayer. In the coculture models, anti-TGF-β1 antibody (10 μg/ml) increased the permeability coefficient of Na-F for MBEC4 cells from 86.7 ± 6.1 to 101.7 ± 9.1% of the control value (vehicle-treated MBEC4 monolayer) and the accumulation of rhodamine 123 in MBEC4 cells from 76.6 ± 6.5 to 90.1 ± 8.0% of the control value (Fig. 3). For the permeability to Na-F (Fig. 3A), a two-way ANOVA showed significant effects for the factors culture system (monolayer and coculture) [$F(1, 25) = 4.65$, $P < 0.05$], treatment (vehicle and antibody) [$F(1, 25) = 8.25$, $P < 0.01$] and interaction (culture system × treatment) [$F(1, 25) = 11.51$, $P < 0.005$]. For accumulation of rhodamine 123 (Fig. 3B), a two-way ANOVA showed

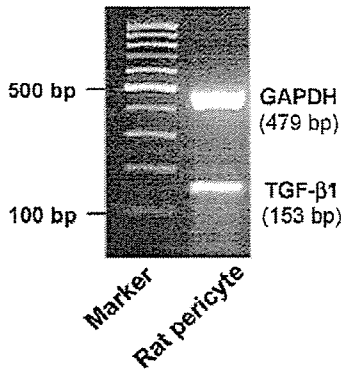


Fig. 2. TGF-β1 mRNA expression in rat pericytes detected by RT-PCR analysis. RNA samples from rat pericytes were used for RT-PCR with primer pairs specific for rat TGF-β1 and GAPDH.

significant effects for culture system [$F(1, 18) = 14.88$, $P < 0.005$] and interaction [$F(1, 18) = 11.97$, $P < 0.005$], but not for treatment. Tukey–Kramer post hoc tests indicated that anti-TGF-β1 antibody significantly increased the permeability to Na-F ($P < 0.01$) and the accumulation of rhodamine 123 in MBEC4 cells ($P < 0.05$) in the coculture system, but not in the monolayer (Fig. 3).

A 12-h exposure to SB431542 (10 μM) significantly increased the permeability from 73.8 ± 3.4 to 87.6 ± 3.9% and moderately elevated the accumulation of rhodamine 123 in MBEC4 cells from 79.0 ± 8.4 to 91.7 ± 11.6% of the control value in the opposite coculture system (Fig. 4). For permeability to Na-F (Fig. 4A), a two-way ANOVA showed significant effects for the factors culture system [$F(1, 21) = 90.10$, $P < 0.0001$], treatment [$F(1, 21) = 14.21$, $P < 0.005$] and interaction [$F(1, 21) = 6.73$, $P < 0.05$]. For the accumulation of rhodamine 123 (Fig. 4B), a two-way ANOVA showed significant effects for culture system [$F(1, 32) = 13.18$, $P < 0.001$] and interaction [$F(1, 32) = 4.16$, $P < 0.05$], but not for treatment. Tukey–Kramer post hoc tests indicated that SB431542 significantly increased the permeability to Na-F ($P < 0.01$) in the coculture system, but not in the MBEC4 monolayer.

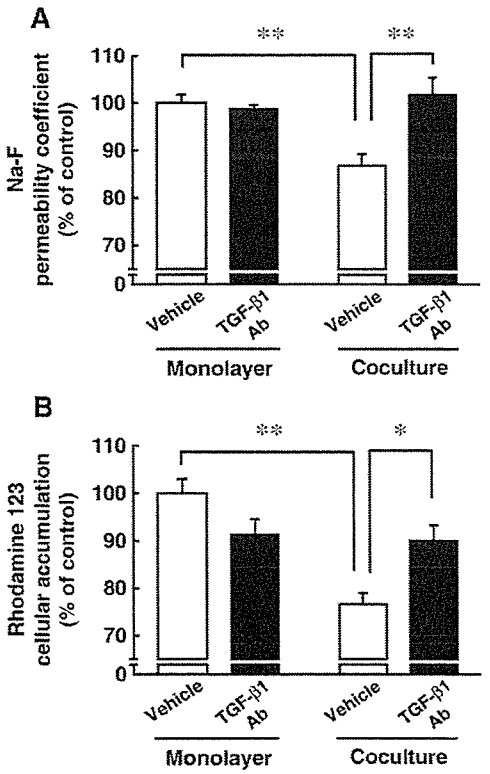


Fig. 3. Effect of anti-TGF-β1 antibody on MBEC4 permeability (A) and P-gp function of MBEC4 cells (B) in the MBEC4 monolayer and rat pericyte coculture systems. Experiments were performed after 12 h of exposure to anti-TGF-β1 antibody (TGF-β1 Ab; 10 μg/ml). (A) MBEC4 permeability coefficients of Na-F. Results are expressed as a percentage of the control (vehicle-treated MBEC4 monolayers) value ($3.85 \pm 0.11 \times 10^{-4}$ cm/min). Values are the means ± SEM ($n = 6$–11). $^{**}P < 0.01$. (B) Rhodamine 123 accumulation in MBEC4 cells. Results are expressed as a percentage of the control value (2.46 ± 0.08 nmol/mg protein). Values are the mean ± SEM ($n = 3$–7). $^{*}P < 0.05$, $^{**}P < 0.01$.

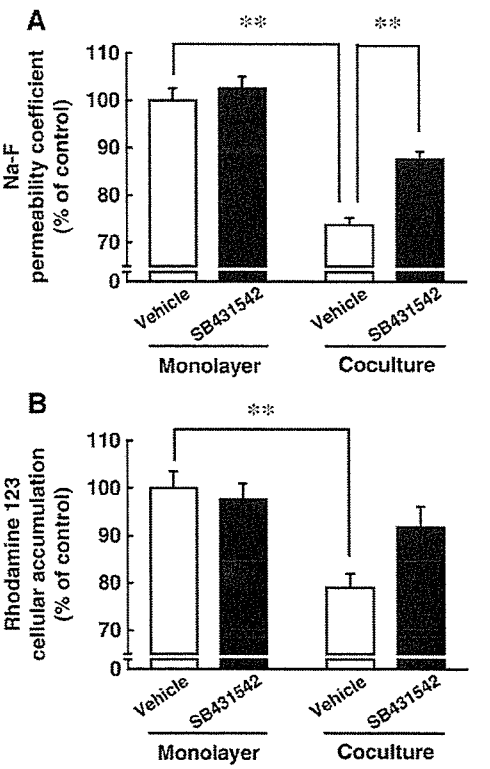


Fig. 4. Effect of a TGF-β type I receptor inhibitor (SB431542) on MBEC4 permeability (A) and P-gp function of MBEC4 cells (B) in the MBEC4 monolayer and rat pericyte coculture systems. Experiments were performed after 12 h of exposure to SB431542 (10 μM). (A) MBEC4 permeability coefficients of Na-F. Results are expressed as a percentage of the control (vehicle-treated MBEC4 monolayers) value ($4.29 \pm 0.18 \times 10^{-4}$ cm/min). Values are the means ± SEM ($n = 4$–8). $^{**}P < 0.01$. (B) Rhodamine 123 accumulation in MBEC4 cells. Results are expressed as a percentage of the control value (2.22 ± 0.43 nmol/mg protein). Values are the mean ± SEM ($n = 7$–12). $^{**}P < 0.01$.

### 3.3. Effect of TGF-β type I receptor antagonist on TGF-β1-induced enhancement of BBB functions in MBEC4 monolayer

To determine whether the site of treatment had an effect on the permeability of MBEC4 cells, TGF-β1 (10 ng/ml) was applied to the luminal or abluminal side of the MBEC4 monolayer. A 12-h exposure to TGF-β1, when injected into either the luminal or abluminal side, produced significant decreases with the same change in permeability to Na-F (35.7 and 36.6%, respectively) (Fig. 5). Then, TGF-β1 and the TGF-β1 receptor antagonist were applied to the luminal compartment of the MBEC4 monolayer.

The TGF-β1 antagonist SB431542 (10 μM) alone had no effect on the permeability to Na-F and the accumulation of rhodamine 123 in the MBEC4 monolayer. TGF-β1 (1 ng/ml) significantly decreased the permeability ($P < 0.01$ vs. vehicle) and accumulation of rhodamine 123 in MBEC4 cells ($P < 0.01$ vs. vehicle). SB431542 (10 μM) completely blocked the TGF-β1-induced decreases in permeability (106.5 ± 2.2% of vehicle, $P < 0.01$ vs. TGF-β1) and accumulation of rhodamine 123 (107.4 ± 4.0% of vehicle, $P < 0.01$ vs. TGF-β1) (Fig. 6).

## 4. Discussion

The present study demonstrated that pericytes positively retain BBB functioning through contact with brain endothelial cells and a soluble factor secreted from pericytes. We made three in vitro BBB models; the MBEC4 monolayer, rat pericyte coculture (bottom) and rat pericyte coculture (opposite) (Fig. 1). The pericyte-released substances are permitted to interact with brain endothelial cells through the pores of the insert (0.4 μm pore size) in the bottom coculture model. The opposite coculture model produces a partial contact effect in addition to the soluble factor from pericytes. In the presence of rat pericytes, the permeability to Na-F and the accumulation of rhodamine 123 in MBEC4 cells were markedly decreased (Fig. 1). A positive role for

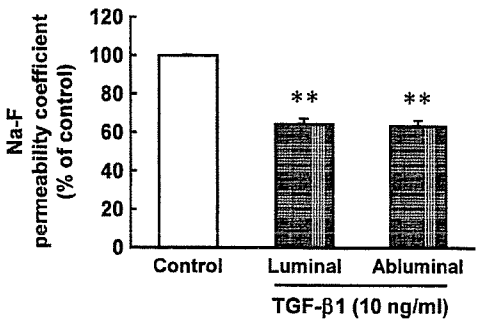


Fig. 5. Functional polarity to the permeability effect of TGF-β1 in MBEC4 monolayers. MBEC4 monolayers were exposed to TGF-β1 (10 ng/ml, 12 h) on either the luminal or abluminal side. The permeability coefficient of Na-F for the control was 2.51 ± 0.02 × $10^{-4}$ cm/min. Values are the mean ± SEM ($n = 4$). **$P < 0.01$, significant difference from control.

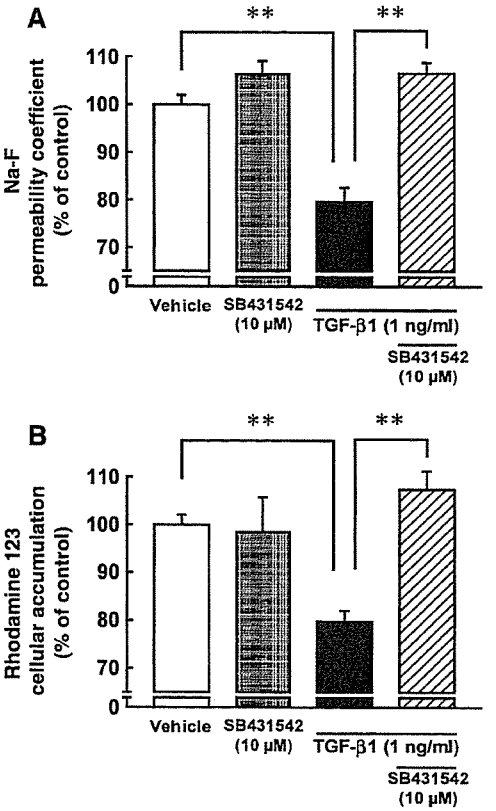


Fig. 6. Effect of a TGF-β type I receptor inhibitor (SB431542) on TGF-β1-enhanced tightening of paracellular junctions (A) and P-gp function of MBEC4 cells (B) in MBEC4 monolayers. Experiments were performed after 12 h of exposure to TGF-β1 (1 ng/ml) and/or SB431542 (10 μM). (A) MBEC4 permeability coefficients of Na-F. Results are expressed as a percentage of the control value (3.66 ± 0.25 × $10^{-4}$ cm/min). Values are the mean ± SEM ($n$ = 8–12). **$P < 0.01$. (B) Rhodamine 123 accumulation in MBEC4 cells. Results are expressed as a percentage of the control value (1.14 ± 0.02 nmol/mg protein). Values are the mean ± SEM ($n$ = 3–4). **$P < 0.01$.

pericytes in the expression and maintenance of endothelial tight junctions has been documented [13,15], although there are few reports concerning pericyte-enhanced P-gp function. Pericytes in the opposite coculture system apparently enhanced BBB properties compared to those in the bottom coculture model (Fig. 1). These findings suggest that pericytes participate in tightening the intercellular junctions and facilitating P-gp function in brain endothelial cells through the production of soluble factors and cell-to-cell contact. Therefore, we employed the opposite coculture model to investigate effects of the inhibition of TGF-β1 signaling on BBB functions in rat pericyte cocultures.

The anti-TGF-β1 antibody and TGF-β1 receptor antagonist (SB431542) were used here at the maximal concentration having no significant effect on BBB functions in the MBEC4 monolayer. Anti-TGF-β1 antibody reversed the decrease in permeability to Na-F and in the accumulation of rhodamine 123 in the rat pericyte coculture to the corresponding levels in the MBEC4 monolayer (Fig. 3). TGF-β1 receptor antagonist (SB431542) inhibited pericyte-

induced decreases in the permeability to Na-F and the accumulation of rhodamine 123 in MBEC4 cells by 50–60% (Fig. 4). A longer period of exposure than 12 h and/or an injection before 3 days may need to be tested. The present results suggest that the pericyte-induced enhancement of BBB functions is mediated to some extent by TGF-β1. RT-PCR analysis of rat pericytes demonstrated the expression of TGF-β1 (Fig. 2). It is, therefore, conceivable that pericyte-derived soluble factors include TGF-β1 and enhance both tight junctions and P-gp function through, at least in part, the TGF-β type I receptor. This notion is supported by our previous findings that TGF-β1 actually lowers the endothelial permeability and enhances the functional activity of P-gp [8]. In the present study, effects of TGF-β1 adsorption and TGF-β receptor inhibition emerged within 12 h (Figs. 3 and 4), after brain pericytes had induced a restoration of the BBB properties of MBEC4 cells. Thus, brain pericytes seem to positively maintain BBB functioning by continuously producing TGF-β1.

TGF-β expresses its physiological actions predominantly through two types of receptors with serine/threonine kinase activity, TGF-β type I and II receptors [20]. The binding of TGF-β to the TGF-β type II receptor induces the assembly of the TGF-β type I receptor-type II receptor heterodimer, leading to phosphorylation of TGF-β type I induced by the type II receptor. As shown in Fig. 6, SB431542 (10 μM) significantly inhibited the TGF-β1-induced enhancement of BBB functions in the MBEC4 monolayer, suggesting that TGF-β1 facilitates the barrier function of the BBB through the TGF-β type I receptor. It is, therefore, likely that the activation of the TGF-β1/TGF-β receptor pathway between brain endothelial cells and brain pericytes contributes to an enhancement of the tight junctions and P-gp function. Mouse brain capillary endothelial cells expressed TGF-β type I and II receptors [9]. The TGF-β type I receptor was expressed on blood vessels of the basal surface of endothelial cells [9]. In the present study, the enhancement of the permeability and P-gp function of MBEC4 cells induced by TGF-β1 (10 ng/ml) was not dependent on addition to the luminal (blood) or the abluminal (brain) side (Fig. 5). These findings suggest that the TGF-β receptor may be located on both sides of MBEC4 cells. The possibility that TGF-β1 injected into the abluminal compartment is transported in the luminal side through MBEC4 cells could not be excluded. The TGF-β signaling cascades from membrane to nucleus including MAPK and a receptor serine/threonine kinase pathway are probably involved in the enhancement of BBB functions. It is, therefore, conceivable that TGF-β facilitates the barrier function and P-gp functional activity of brain endothelial cells by increasing the expression of tight junction-associated proteins (such as occludin and claudins) and P-gp. The signal molecules involved in the enhancement of BBB functions following the activation of TGF-β1/TGF-β receptor pathway are now under investigation.

In several neurodegenerative diseases, changes in BBB functions and an increase of TGF-β1 in the brain have been described [11,16]. However, it has not been determined whether the increase in the expression of TGF-β observed in human neurodegenerative diseases is the underlying cause or the result of degenerative conditions. Thus, TGF-β1 seems to protect against impairment of the BBB and positively maintain brain homeostasis. In fact, the degeneration of pericytes was observed in neurodegenerative diseases [19,30]. This phenomenon probably decreases TGF-β production, leading to dysfunction of the BBB.

Other soluble factors derived from pericytes, VEGF and bFGF, were reported to influence BBB functions. VEGF increased the permeability of brain endothelial cells, suggesting that VEGF is a barrier-weakening factor [31]. bFGF was found to tighten the intercellular junctions and induce the expression of multidrug resistance proteins [26]. TGF-β1 up-regulated the induction of bFGF production [10]. Angiopoietin-1, an antipermeability factor [18] secreted from pericytes, produced the expression of occludin mRNA in brain endothelial cells [15]. It is, therefore, conceivable that brain pericytes regulate BBB functions by secreting these substances. TGF-β1, VEGF, bFGF and angiopoietin-1 appear to be involved in the interaction of endothelial cells, pericytes and astrocytes under physiological and pathophysiological conditions, since these substances are also produced by astrocytes.

In conclusion, brain pericytes induce and up-regulate the barrier function and P-gp functional activity of brain endothelial cells. This pericyte-induced up-regulation of BBB functions is mediated, at least in part, through continuous TGF-β production.

## Acknowledgments

This work was supported, in part, by Grants-in-Aid for Scientific Research ((B)(2) 14370789) and ((C)(2) 15590475) from JSPS, Japan, by a Grant-in-Aid for Exploratory Research (16659138) from MEXT, Japan, and by funds (No. 031001) from the Central Research Institute of Fukuoka University and MEXT. HAITEKU (2000-2004). The authors thank Dr. Mária A. Deli, Institute of Biophysics, Biological Research Centre of the Hungarian Academy of Sciences for important comments on the preparation of the primary culture of pericytes.

## References

[1] A. Antonelli-Orlidge, K.B. Saunders, S.R. Smith, P.A. D'Amore, An activated form of transforming growth factor β is produced by cocultures of endothelial cells and pericytes, Proc. Natl. Acad. Sci. U. S. A. 88 (1989) 4544–4548.

[2] R. Balabanov, P. Dore-Duffy, Role of the CNS microvascular pericyte in the blood–brain barrier, J. Neurosci. Res. 53 (1998) 637–644.

[3] V. Berezowski, C. Landry, M.-P. Dehouck, R. Cecchelli, L. Fenart, Contribution of glial cells and pericytes to the mRNA profiles of P-glycoprotein and multidrug resistance-associated proteins in an in vitro model of the blood–brain barrier, Brain Res. 1018 (2004) 1–9.
[4] M.M. Bradford, A rapid and sensitive method for the quantitation of microgram quantities of protein utilizing the principle of protein-dye binding, Anal. Biochem. 72 (1976) 248–254.
[5] M.-P. Dehouck, P. Jolliet-Riant, F. Brée, J.-C. Fruchart, R. Cecchelli, J.P. Tillement, Drug transfer across the blood–brain barrier: correlation between in vitro and in vivo models, J. Neurochem. 58 (1992) 1790–1797.
[6] R. Derynck, Y.E. Zhang, Smad-dependent and Smad-independent pathways in TGF-β family signaling, Nature 425 (2003) 577–584.
[7] S. Dohgu, Y. Kataoka, H. Ikesue, M. Naito, T. Tsuruo, R. Oishi, Y. Sawada, Involvement of glial cells in cyclosporine-increased permeability of brain endothelial cells, Cell. Mol. Neurobiol. 20 (2000) 781–786.
[8] S. Dohgu, A. Yamauchi, F. Takata, M. Naito, T. Tsuruo, S. Higuchi, Y. Sawada, Y. Kataoka, Transforming growth factor-β1 upregulates the tight junction and P-glycoprotein of brain microvascular endothelial cells, Cell. Mol. Neurobiol. 24 (2004) 491–497.
[9] D.B. Fee, D.L. Sewell, K. Andresen, T.J. Jacques, S. Piaskowski, B.A. Barger, M.N. Hart, Z. Fabry, Traumatic brain injury increases TGFβRII expression on endothelial cells, Brain Res. 1012 (2004) 52–59.
[10] G.A. Finlay, V.J. Thannickal, B.L. Fanburg, K.E. Paulson, Transforming growth factor-β1-induced activation of the ERK pathway/activator protein-1 in human lung fibroblasts requires the autocrine induction of basic fibroblast growth factor, J. Biol. Chem. 275 (2000) 27650–27656.
[11] K.C. Flanders, R.F. Ren, C.P. Lippa, Transforming growth factor-βs in neurodegenerative disease, Prog. Neurobiol. 54 (1998) 71–85.
[12] M. Fontaine, W.F. Elmquist, D.W. Miller, Use of rhodamine 123 to examine the functional activity of P-glycoprotein in primary cultured brain microvessel endothelial cell monolayers, Life Sci. 59 (1996) 1521–1531.
[13] K. Hayashi, S. Nakao, R. Nakaoke, S. Nakagawa, N. Kitagawa, M. Niwa, Effects of hypoxia on endothelial/pericytic co-culture model of the blood–brain barrier, Regul. Pept. 123 (2004) 77–83.
[14] K.K. Hirashi, P.A. D'Amore, Pericyte in the microvasculature, Cardiovasc. Res. 32 (1997) 687–698.
[15] S. Hori, S. Ohtsuki, K. Hosoya, E. Nakashima, T. Terasaki, A pericyte-derived angiopoietin-1 multimeric complex induces occludin gene expression in brain capillary endothelial cells through Tie-2 activation in vitro, J. Neurochem. 89 (2004) 503–513.
[16] J.D. Huber, R.D. Egleton, T.P. Davis, Molecular physiology and pathophysiology of tight junctions in the blood–brain barrier, Trends Neurosci. 24 (2001) 719–725.
[17] Y. Kim, R.Y. Imdad, A.H. Stephanson, R.S. Sprague, A.J. Lonigro, Vascular endothelial growth factor mRNA in pericytes is upregulated by phorbol myristate acetate, Hypertension 31 (1998) 511–515.
[18] S.W. Lee, W.J. Kim, Y.K. Choi, H.S. Song, H.S. Son, M.J. Son, I.H. Gelman, Y.J. Kim, K.W. Kim, SSeCKS regulates angiogenesis and tight junction formation in blood–brain barrier, Nat. Med. 9 (2003) 900–906.
[19] B.H. Liwnicz, J.L. Leach, H.-S. Yeh, M. Privitera, Pericyte degeneration and thickening of basement membranes of cerebral microvessels in complex parcial seizures: electron microscopic study of surgically removed tissue, Neurosurgery 26 (1997) 409–420.
[20] J. Massagué, TGF-β signal transduction, Annu. Rev. Biochem. 67 (1998) 753–791.
[21] A. Orlidge, P.A. D'Amore, Inhibition of capillary endothelial cell growth by pericytes and smooth muscle cells, J. Cell Biol. 105 (1987) 1455–1462.
[22] M. Ramsauer, D. Krause, R. Dermietzel, Angiogenesis of the blood–brain barrier in vitro and the function of cerebral pericytes, FASEB J. 16 (2002) 1274–1276.
[23] L.L. Rubin, J.M. Staddon, The cell biology of the blood–brain barrier, Annu. Rev. Neurosci. 22 (1999) 11–28.
[24] H.K. Rucker, H.J. Wynder, W.E. Thomas, Cellular mechanisms of CNS pericytes, Brain Res. Bull. 51 (2000) 363–369.
[25] Y. Sato, D.B. Rifkin, Inhibition of endothelial cell movement by pericytes and smooth muscle cells: activation of a latent transforming growth factor-β1-like molecular by plasmin during co-culture, J. Cell Biol. 109 (1989) 309–315.
[26] K. Sobue, N. Yamamoto, K. Yoneda, M.E. Hodgson, K. Yamashiro, N. Tsuruoka, T. Tsuda, H. Katsuya, Y. Miura, K. Asai, T. Kato, Induction of blood–brain barrier properties in immortalized bovine brain endothelial cells by astrocytic factors, Neurosci. Res. 35 (1999) 155–164.
[27] C.A. Szabó, M.A. Deli, T.K.D. Ngo, F. Joó, Production of pure primary rat cerebral endothelial cell culture: a comparison of different methods, Neurobiology 5 (1997) 1–16.
[28] T. Tatsuta, M. Naito, T. Oh-hara, I. Sugawara, T. Tsuruo, Functional involvement of P-glycoprotein in blood–brain barrier, J. Biol. Chem. 267 (1992) 20383–20391.
[29] T. Tatsuta, M. Naito, K. Mikami, T. Tsuruo, Enhanced expression by the brain matrix of P-glycoprotein in brain capillary endothelial cells, Cell Growth Differ. 5 (1994) 1145–1152.
[30] M.M. Verbeek, R.M. de Waal, J.J. Schipper, W.E. Van Nostrand, Rapid degeneration of cultured human brain pericytes by amyloid beta protein, J. Neurochem. 68 (1997) 1135–1141.
[31] W. Wang, M.J. Merrill, R.T. Borchardt, Vascular endothelial growth factor affects permeability of brain microvessel endothelial cells in vitro, Am. J. Physiol. 271 (1996) C1973–C1980.

HIGH LIGHT CME

# Clinical diagnosis of MM2-type sporadic Creutzfeldt–Jakob disease

T. Hamaguchi, MD; T. Kitamoto, MD, PhD; T. Sato, MD, PhD; H. Mizusawa, MD, PhD; Y. Nakamura, MD, MPH, FFPHM; M. Noguchi, MD; Y. Furukawa, MD; C. Ishida, MD, PhD; I. Kuji, MD, PhD; K. Mitani, MD; S. Murayama, MD, PhD; T. Kohriyama, MD, PhD; S. Katayama, MD, PhD; M. Yamashita, MD, PhD; T. Yamamoto, MD, PhD; F. Udaka, MD, PhD; A. Kawakami, MD, PhD; Y. Ihara, MD, PhD; T. Nishinaka, MD, PhD; S. Kuroda, MD, PhD; N. Suzuki, MD; Y. Shiga, MD, PhD; H. Arai, MD, PhD; M. Maruyama, MD, PhD; and M. Yamada, MD, PhD

**Abstract**—*Background:* No method for the clinical diagnosis of MM2-type sporadic Creutzfeldt–Jakob disease (sCJD) has been established except for pathologic examination. *Objective:* To identify a reliable marker for the clinical diagnosis of MM2-type sCJD. *Methods:* CSF, EEG, and neuroimaging studies were performed in eight patients with MM2-type sCJD confirmed by neuropathologic, genetic, and western blot analyses. *Results:* The eight cases were pathologically classified into the cortical (n = 2), thalamic (n = 5), and combined (corticothalamic) (n = 1) forms. The cortical form was characterized by late-onset, slowly progressive dementia, cortical hyperintensity signals on diffusion-weighted imaging (DWI) of brain, and elevated levels of CSF 14-3-3 protein. The thalamic form showed various neurologic manifestations including dementia, ataxia, and pyramidal and extrapyramidal signs with onset at various ages and relatively long disease duration. Characteristic EEG and MRI abnormalities were almost absent. However, all four patients examined with cerebral blood flow (CBF) study using SPECT showed reduction of the CBF in the thalamus as well as the cerebral cortex. The combined form had features of both the cortical and the thalamic forms, showing cortical hyperintensity signals on DWI and hypometabolism of the thalamus on [$^{18}$F]2-fluoro-2-deoxy-D-glucose PET. *Conclusion:* For the clinical diagnosis of MM2-type sporadic Creutzfeldt–Jakob disease, cortical hyperintensity signals on diffusion-weighted MRI are useful for the cortical form and thalamic hypoperfusion or hypometabolism on cerebral blood flow SPECT or [$^{18}$F]2-fluoro-2-deoxy-D-glucose PET for the thalamic form.

NEUROLOGY 2005;64:643–648

Sporadic Creutzfeldt–Jakob disease (sCJD) has been classified based on the genotype at polymorphic codon 129 of the prion protein gene (*PrP*) and the physicochemical properties of the pathologic PrP ($PrP^{Sc}$); various classification systems have been proposed.[1-5] A simple classification[1,2] has been widely accepted and recognizes at least six phenotypes in sCJD: MM1, MV1, VV1, MM2, MV2, and VV2.[3] About 70% of patients with sCJD show the classic CJD phenotype and are mostly classified as MM1 or MV1 types.[3] Their clinical diagnosis relies on the detection of periodic sharp-wave complexes (PSWCs) in EEG, elevated levels of CSF 14-3-3 protein, and typical hyperintensity signals of brain MRI in addition to the classic clinical manifestations.[3,6]

Other phenotypes of sCJD do not present with typical clinical symptoms of classic CJD or PSWCs on EEG.[3,6] Both VV2 and MV2 patients are characterized by ataxia and dementia,[3] and brain MRI and CSF 14-3-3 protein are useful for their clinical diagnosis.[6] As for several reported patients with MM2-type sCJD, some showed positive CSF 14-3-3 protein, but others did not.[6-9] Thus, for MM2 as well as VV1, diagnostic markers have not been established yet.

The clinical features of MM2-type sCJD in some patients were previously reported.[1,3,6,8,10,11] MM2-type sCJD presents with at least two pathologic phenotypes: MM2 cortical and MM2 thalamic forms.[3] In the MM2 cortical phenotype, dementia is a major symptom, and visual or cerebellar signs are usually

From the Department of Neurology and Neurobiology of Aging (Drs. Hamaguchi, Noguchi, Furukawa, and Yamada), Kanazawa University Graduate School of Medical Science, Departments of Neurological Science (Dr. Kitamoto), Neurology (Drs. Suzuki and Shiga), and Geriatric and Complementary Medicine (Drs. Arai and Maruyama), Tohoku University Graduate School of Medicine, Sendai, National Center for Neurology and Psychiatry (Dr. Sato), Kohnodai Hospital, Ichikawa, Department of Neurology and Neurological Science (Dr. Mizusawa), Graduate School, Tokyo Medical and Dental University, Department of Public Health (Dr. Nakamura), Jichi Medical School, Minamikawachi, Department of Neurology (Dr. Ishida), Noto General Hospital, Nanao, Department of Nuclear Medicine (Dr. Kuji), Kanazawa University Hospital, Department of Neurology (Dr. Mitani), Tokyo Metropolitan Geriatric Medical Center, Department of Neuropathology (Dr. Murayama), Tokyo Metropolitan Institute of Gerontology, Department of Neurology (Drs. Kohriyama and Katayama), Hiroshima University Hospital, Department of Neurology (Drs. Yamashita and Yamamoto), Saiseikai Nakatsu Hospital and Medical Center, Osaka, Department of Neurology (Dr. Udaka), Sumitomo Hospital, Osaka, Department of Neurology (Dr. Kawakami), Kaetsu Hospital, Niitsu, Department of Neurology (Drs. Ihara and Nishinaka), Clinical Research Institute, National Hospital Organization Minami-Okayama Medical Center, Okayama, Department of Neuropsychiatry (Dr. Kuroda), Okayama University Graduate School of Medicine and Dentistry, and Creutzfeldt–Jakob Disease Surveillance Committee (Drs. Kitamoto, Sato, Mizusawa, Nakamura, Murayama, Kuroda, Shiga, and Yamada), Japan.

Supported in part by a grant from the Research Committee on Prion Diseases and Slow Virus Infection, Ministry of Health, Welfare, and Labor, Japan.

Received May 24, 2004. Accepted in final form November 1, 2004.

Address correspondence and reprint requests to Dr. M. Yamada, Department of Neurology and Neurobiology of Aging, Kanazawa University Graduate School of Medical Science, 13-1, Takara-machi, Kanazawa 920-8640, Japan; e-mail: m-yamada@med.kanazawa-u.ac.jp

 

*Table 1* *Clinical features of eight patients with MM2-type sCJD*

| Patient no. | Sex | Onset, y | Course, mo | Onset symptoms | Clinical manifestations during illness | Initial diagnosis |
|---|---|---|---|---|---|---|
| 1 | F | 65 | Alive (13) | Dementia | Dementia, pyramidal signs, insomnia | CJD |
| 2 | F | 75 | Alive (28) | Depression | Psychiatric symptoms, dementia, myoclonus | CJD |
| 3 | M | 65 | 14 | Falling to left side | Dementia, myoclonus, cerebellar ataxia, akinetic mutism | CJD |
| 4 | F | 49 | 30 | Insomnia | Insomnia, dementia, psychiatric symptoms, pyramidal signs, extrapyramidal signs, autonomic symptoms, myoclonus, akinetic mutism | PSP |
| 5 | M | 64 | 53 | Photophobia | Visual symptoms, extrapyramidal signs, dementia, autonomic symptoms, psychiatric symptoms, myoclonus, akinetic mutism | PSP |
| 6 | F | 30 | 73 | Blurred vision | Visual symptoms, psychiatric symptoms, cerebellar ataxia, dementia, pyramidal signs, extrapyramidal signs, myoclonus, akinetic mutism | SCD |
| 7 | M | 71 | 25 | Ataxic gait | Cerebellar ataxia, autonomic symptoms, dementia | SCD |
| 8 | M | 58 | 13 | Dementia | Dementia, cerebellar ataxia, myoclonus, pyramidal signs, psychiatric symptoms | AD |

sCJD = sporadic Creutzfeldt–Jakob disease; PSP = progressive supranuclear palsy; SCD = spinocerebellar degeneration; AD = Alzheimer disease.

absent.[3] There have been no reports of laboratory or neuroimaging studies in MM2 cortical sCJD. In the MM2 thalamic phenotype, the clinical features are insomnia and psychomotor hyperactivity in addition to ataxia and cognitive impairment.[3] This phenotype may be called sporadic fatal insomnia (SFI) because the clinical and pathologic features resemble those of fatal familial insomnia (FFI).[8,10] In the MM2 thalamic form or SFI, no PSWCs on EEG, positive or negative 14-3-3 protein in CSF, and normal brain MRI have been reported.[6,8,10]

Since a report of variant CJD (vCJD) in the United Kingdom in 1996,[12] identification of vCJD has been an important part of the surveillance of prion diseases. The clinical features of vCJD are similar to those of MM2-type sCJD, including young age at onset, long disease duration, absence of PSWCs on EEG, and methionine homozygosity on codon 129 of *PrP* gene.[3,13] Therefore, MM2-type sCJD is important in the differential diagnosis for vCJD.

We have investigated the clinical and neuroimaging features of eight patients with MM2-type sCJD in an attempt to identify a reliable marker for the clinical diagnosis of this type of sCJD.

**Methods.** *Subjects.* We investigated eight patients with MM2-type sCJD confirmed by neuropathologic, genetic, and western blot analyses. The clinical features, results of EEG, CSF 14-3-3 protein, MRI, cerebral blood flow (CBF) studies using SPECT, and brain glucose metabolism studies using [$^{18}$F]2-fluoro-2-deoxy-D-glucose (FDG) PET were reviewed. CBF-SPECT using $^{99m}$Tc-ethyl cysteinate dimer ($^{99m}$Tc-ECD) was performed in three (Patients 1, 2, and 8), CBF-SPECT using *N*-isopropyl-*p*-[$^{123}$I]iodoamphetamine in three (Patients 4, 5, and 6), and FDG-PET in one (Patient 3). MRI, CBF-SPECT, and FDG-PET were evaluated by two neurologists and a neuroradiologist without knowledge of the clinical findings. None of these subjects had a family history of CJD or known exposure to prion contamination in the past.

*Analysis of* PrP *gene.* DNA was extracted from the blood, and the open reading frame of the *PrP* gene was analyzed as previously described.[14,15]

*Neuropathology.* The brain tissues were obtained by brain biopsy (Patients 1 and 2) or autopsy (Patients 3 to 8). Brain tissue sections were stained with routine neuropathologic techniques. Immunohistochemistry was performed with a monoclonal antibody to PrP (3F4), as previously described.[16]

*Western blot analysis.* Brain tissue from the frontal lobe was homogenized, and western blot analysis of protease K-resistant PrP was performed with 3F4 as previously described.[17]

**Results.** *Clinical features and laboratory and neuroimaging studies.* The clinical features are summarized in table 1 and the laboratory and neuroimaging studies in table 2. The details of the clinical and pathologic features of Patients 5[18] and 6[11] were previously reported, and Patient 8 was included in a previous MRI study.[19] The details of the clinical features of three representative patients (Patients 2, 3, and 8) are described below.

*Patient 2.* A 75-year-old woman developed forgetfulness and depression. Her mental symptoms gradually deteriorated, and she was admitted to our hospital 14 months after the onset. Neurologically, she showed only dementia (Mini-Mental State Examination 9/30) with depressed mood.

Sixteen months after the onset, the MRI showed gyriform hyperintensity in the bilateral frontal, temporal, parietal, and occipital cortices on diffusion-weighted imaging (DWI) (figure 1A). Less intense and smaller cortical lesions were shown on fluid-attenuated inversion recovery imaging (see figure 1B). On the EEG, diffuse slowing was found without PSWCs. CBF-SPECT using $^{99m}$Tc-ECD showed re-

*Table 2 Laboratory and neuroimaging findings of eight patients with MM2-type sCJD*

| | EEG | | | CSF | | Abnormal signals on MRI* | | | | Reduction of CBF or hypometabolism | | | |
|---|---|---|---|---|---|---|---|---|---|---|---|---|---|
| Patient no. | Slowing | PSWCs | DD, mo | 14-3-3 | DD, mo | CO | BG | TH | DD, mo | CO | BG | TH | DD, mo |
| 1 | + | − | 13 | + | 9 | + | − | − | 7 | + | − | − | 9 |
| 2 | + | + | 27 | + | 16 | + | − | − | 16 | + | − | − | 16 |
| 3 | + | − | 11 | ± | 4 | + | − | − | 4 | + | − | + | 4 |
| 4 | + | − | 25 | NA | | NA | | | | + | − | + | 16 |
| 5 | + | − | 42 | NA | | NA | | | | + | − | + | 12 |
| 6 | + | + | 36 | NA | | − | − | − | 58 | + | − | + | 37 |
| 7 | + | − | 9 | + | 9 | − | − | − | 13 | NA | | | |
| 8 | + | − | 7 | ± | 7 | − | − | − | 7 | + | − | + | 7 |

sCJD = sporadic Creutzfeldt–Jakob disease; CBF = cerebral blood flow; PSWCs = periodic sharp-wave complexes; DD = disease duration at time point when each examination showed the following results: PSWCs on EEG, positive 14-3-3 protein in CSF, abnormal signals on MRI, and reduction of CBF on SPECT or hypometabolism on [$^{18}$F]2-fluoro-2-deoxy-D-glucose PET or at the time when the last examination was performed if the examinations revealed negative results throughout the clinical course; CO = cortex; BG = basal ganglia; TH = thalamus.

* We judge that abnormal signals are positive on MRI when they are shown on any sequence, such as T1-weighted, T2-weighted, diffusion-weighted, and fluid-attenuated inversion recovery images.

duction of the CBF in the bilateral parietal and temporal cortices (figure 2A). CSF examination revealed an increased level of 14-3-3 protein (28 ng/mL [normal <20 ng/mL]). Although the clinical criteria of sCJD[20] were not fulfilled because of the scarcity of neurologic and EEG abnormalities, CJD was suspected on the basis of MRI and CSF findings.

Twenty-seven months after the onset, the EEG showed PSWCs. Cortical hyperintensity signals on DWI were found to extend to the bilateral frontal regions. $^{99m}$Tc-ECD SPECT showed diffuse severe reduction of CBF except in the cerebellum, basal ganglia, and thalamus. To confirm the diagnosis of CJD for participation in a clinical trial of pentosan polysulfate, brain biopsy of the right frontal lobe was performed with her family's consent 28 months after the onset. The patient developed myoclonic movement involving the bilateral hands and was alive 30 months after the onset.

*Patient 3.* A 65-year-old man developed unsteadiness with a tendency to fall to the left side. Three months after the onset, he showed gait disturbance and dysarthria.

Neurologic examination 4 months after the onset revealed slurred dysarthria, clumsiness of the left upper and lower extremities, and dementia. The EEG was normal. The CSF level of 14-3-3 protein was equivocal. MRI showed gyriform hyperintensity in the bilateral frontal, temporal, parietal, and occipital cortices on DWI. FDG-PET of the brain showed diffuse hypometabolism in the bilateral thalamus and cortices. CJD was suspected as an initial diagnosis.

Thereafter, the patient's symptoms rapidly progressed; he became bedridden and could not communicate 5 months after the onset. Myoclonus of the extremities developed 9 months after the onset. Eleven months after the onset, cortical lesions with hyperintense signals on DWI extended more widely than in the previous study and revealed diffuse, mild atrophy. EEG revealed diffuse slowing without PSWCs. The CSF level of 14-3-3 protein was still equivocal. The patient fell into akinetic mutism 13 months after the onset. He died 14 months after the onset and was autopsied.

*Patient 8.* A 58-year-old man developed progressive dementia. He showed unsteady gait 5 months after the onset and myoclonic movement in all limbs 6 months after the onset.

Neurologic examination 7 months after the onset revealed dementia, cerebellar ataxia, myoclonic jerking, and exaggerated deep tendon reflexes in all the extremities. Brain MRI, including DWI, and EEG were normal (see figure 1, C and D). CBF-SPECT using $^{99m}$Tc-ECD revealed reduction of the CBF in the bilateral thalamus and cortices of the temporal and parietal lobes (see figure 2B). A CSF study disclosed a mild increase of protein concentration (44 mg/dL) and equivocal levels of 14-3-3 protein. The diagnosis was suspicion of Alzheimer disease (AD).

His symptoms gradually deteriorated. He also developed visual hallucinations and confusion 12 months after the onset. Thirteen months after the onset, he died and was autopsied.

PrP *gene analysis.* Analysis of the *PrP* gene revealed no mutation in any of the eight patients. The polymorphic codons showed methionine homozygosity at codon 129 and glutamic acid homozygosity at codon 219 in all the patients.

*Neuropathology.* Neuropathologically, the biopsy samples from the right frontal cortex of Patients 1 and 2 showed similar pathologic findings: prominent spongiform changes, including large vacuoles, with gliosis, and diffuse granular PrP immunostaining of synaptic type with a perivacuolar pattern.

Autopsies were performed in Patients 3 to 8. The neuropathologic findings of Patients 4 to 8 were similar. Severe neuronal loss and gliosis, but no spongiform changes, were observed in the nuclei of the medial thalamus as well as in the inferior olive. In the thalamus, PrP immunoreactivity was absent in all the patients. In the cerebral cortex, spongiform degeneration was absent in Patient 8 and limited to isolated foci in Patients 4 to 7 mainly in the frontal, pari-